Title	Long period grating cascaded to photonic crystal fiber modal interferometer for simultaneous measurement of temperature and refractive index
Author(s)	Hu, Dora Juan Juan; Lim, Jun Long; Jiang, Meng; Wang, Yixin; Luan, Feng; Shum, Perry Ping; Wei, Huifeng; Tong, Weijun
Citation	Hu, D. J. J., Lim, J. L., Jiang, M., Wang, Y., Luan, F., Shum, P. S., et al. (2012). Long period grating cascaded to photonic crystal fiber modal interferometer for simultaneous measurement of temperature and refractive index. Optics Letters, 37(12), 2283-2285.
Date	2012
URL	http://hdl.handle.net/10220/10978
Rights	© 2012 Optical Society of America. This paper was published in Optics Letters and is made available as an electronic reprint (preprint) with permission of Optical Society of America. The paper can be found at the following official DOI: [http://dx.doi.org/10.1364/OL.37.002283]. One print or electronic copy may be made for personal use only. Systematic or multiple reproduction, distribution to multiple locations via electronic or other means, duplication of any material in this paper for a fee or for commercial purposes, or modification of the content of the paper is prohibited and is subject to penalties under law.

Long period grating cascaded to photonic crystal fiber modal interferometer for simultaneous measurement of temperature and refractive index

Dora Juan Juan Hu,[1,*] Jun Long Lim,[1] Meng Jiang,[2] Yixin Wang,[1] Feng Luan,[2] Perry Ping Shum,[2] Huifeng Wei,[3,4] and Weijun Tong[3,4]

[1]*RF & Optical Department, Institute for Infocomm Research, Agency for Science, Technology and Research, Singapore*

[2]*School of Electrical and Electronic Engineering, Nanyang Technological University, Singapore*

[3]*State Key Laboratory of Optical Fiber and Cable Manufacture Technology, China*

[4]*R & D Center, Yangtze Optical Fiber and Cable Company Ltd., China*

Corresponding author: jjhu@i2r.a-star.edu.sg

We propose and demonstrate a novel and simple dual-parameter measurement scheme based on a cascaded optical fiber device of long-period grating (LPG) and photonic crystal fiber (PCF) modal interferometer. The temperature and refractive index (RI) can be measured simultaneously by monitoring the spectral characteristics of the device. The implemented sensor shows distinctive spectral sensitivities of −30.82 nm/RIU (refractive index unit) and 47.4 pm/°C by the LPG, and 171.96 nm/RIU and 10.4 pm/°C by the PCF modal interferometer. The simultaneous measurement of the temperature and external RI is experimentally demonstrated by the sensor. The temperature shift and RI shift calculated by the sensor matrix agree well with the actual temperature and RI change in the experiment.   © 2012 Optical Society of America

OCIS codes: 060.2310, 060.2370.

The growing demand in the *in situ* monitoring of physical, chemical, and biological parameters drives continuous research efforts and the development of sensor technologies. Owing to such desirable and unique features as immunity to electromagnetic interference, compact size, low cost, reliability, etc., optical fiber sensors have made significant progress in and contributions to various sensing applications. Refractive index (RI) and temperature are important physical parameters in many applications, such as water quality monitoring [1,2], biosensing [3–6], etc. Surface plasmon resonance has been demonstrated to be accurate and promising for biosensing applications through evanescent waves in prism configurations [7–8], but the apparatuses are bulky compared to fiber sensors. In addition, temperature-induced crosstalk is a detrimental factor for the detection. It is therefore highly desirable to realize simultaneous monitoring of RI and temperature to minimize or avoid the crosstalk problem.

Photonic crystal fibers (PCFs) made of a single material were used to make temperature-insensitive devices for RI measurement [9]. However, experiments showed that devices made of single-material silica PCF still suffered from considerable temperature cross-sensitivity [10]. On the other hand, grating-based sensors, i.e., fiber Bragg gratings (FBGs) and long-period gratings (LPGs), are typically used for temperature or RI measurement. The cross-sensitivity of the temperature and RI exhibited in the grating-based sensors requires necessary compensation schemes for practical applications. Various schemes have been proposed to achieve dual-parameter measurement of temperature and RI, such as modified FBGs [11–13], fiber tapers [14], fiber in-line Fabry—Perot cavity [15], LPGs in various configurations [16–18] and LPG deposited on side-polished PCF [19], etc. Although the side-polished PCF was able to enhance the evanescent field

coupling to LPG, the structure was fragile and difficult to handle. Recently, a compact PCF modal interferometer was reported on for external biosensing due to its high external RI sensitivity [6]. Nevertheless, the temperature dependence of the interferometer was neglected in the measurement. The temperature-induced crosstalk could still be a limiting factor to achieve accurate measurement, especially in detecting weak signals of biological events. On the other hand, by cascading the LPG to the PCF modal interferometer, it offers a promising solution for dual-parameter measurement of temperature and RI, which is more efficient than single-parameter measurement. Moreover, it permits both interacting parameters to be individually determined so that the crosstalk problem is addressed. Compared to other schemes, such as two LPG configurations, the proposed scheme has a few advantages. Firstly, the PCF device is much more compact, i.e., only 3 mm in length, making the measurement easier to handle compared to much longer fiber devices. Secondly, the thermal response of PCF is dissimilar to LPG, i.e., the thermal sensitivity difference is significant. Thirdly, the highly sensitive RI response of the PCF has the opposite sign to that of the LPG, making the measurement more effective. To the best of authors' knowledge,
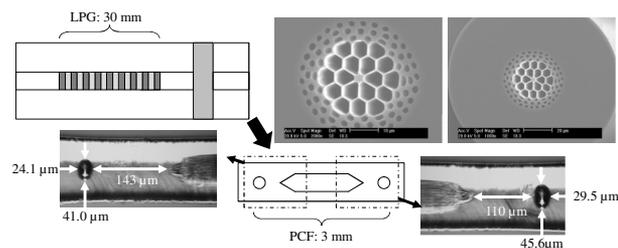

Fig. 1.   Schematic of the cascaded fiber device. The LPG was 30 mm and the PCF was 3 mm. The SEM image of the PCF is shown top right.
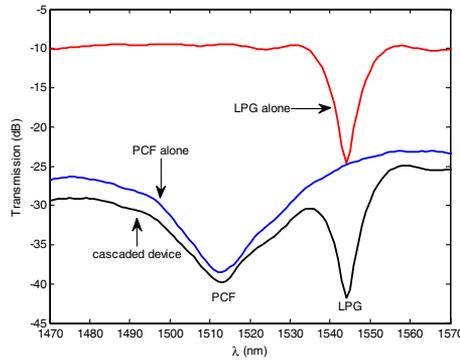
Fig. 2.   (Color online) Spectrum of the cascaded device in DI water under room temperature.

Fig. 4.   Spectral response of the sensor with temperature.

no prior report has demonstrated or investigated this scheme.

The schematic of the cascaded device and the scanning electronic microscopic (SEM) image of the PCF used in the experiment are shown in Fig. 1. The PCF modal interferometer was 3 mm in length and it was fabricated by the microhole collapsing technique, forming a completely collapsed zone and a microbubble in the splice region between single-mode fiber (SMF) and PCF [6]. The PCF had an outer diameter of 123.7 μm. The fully collapsed region was 119 μm in diameter; the length at both sides was 143 and 110 μm. The microbubbles were 24.1×41.0 and 29.5×45.6 μm. The formation of microbubbles was controllable and repeatable with appropriate splicer settings. The device was based on Mach—Zehnder interferometry. The first collapsed region acted as mode splitter to convert part of the core mode to the cladding modes. The microbubble attenuated the core mode and excited more cladding modes, which effectively interacted with the surrounding medium and recombined with the core mode at the second splice region, forming the interference spectrum due to different phase delay [6]. In addition, as confirmed by the high RI sensitivity, the Fabry—Perot cavity effect of the microbubble, which was insensitive to surrounding RI, was not significant compared to the modal interference. A tunable laser source (Agilent 81680A) was used to obtain the spectral information of the sensor. The LPG (30 mm in length) was fabricated by 248 nm excimer laser on hydrogen-loaded SMF with a point-by-point grating writing technique. The grating period was 455 μm. A loss dip of –15 dB at the wavelength of 1546.3 nm was obtained. Figure 2 shows the transmission spectrum of the
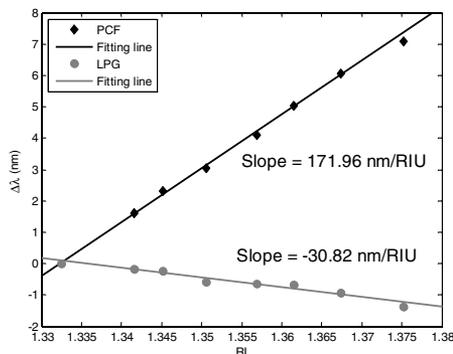
LPG and the PCF device (alone) as well as the cascaded device in deionized (DI) water under room temperature. The resonance wavelengths of LPG and PCF at 1513 nm were well separated to minimize optical crosstalk.

The external RI response was examined by placing the device in glycerin—DI water mix with refractive indices ranging from 1.33 to 1.375 while maintaining the room temperature at 24 °C as shown in Fig. 3. After each test, the sensor was thoroughly rinsed and cleaned by ethanol to remove residual glycerin—DI water mix and dried in air until the spectrum returned to its original spectrum in air. The transmission dip resulted from the LPG and PCF modal interferometer exhibiting distinctive RI responses. As external RI increased, the resonance wavelength of the LPG moved toward shorter wavelengths, whereas the resonance wavelength of the PCF modal interferometer showed red shifts. The sensitivity coefficients were estimated by the linear fitting lines, giving 171.96 nm/RIU (refractive index unit) and –30.82 nm/RIU for PCF and LPG, respectively.

The temperature response of the device was investigated by placing the sensor in an oven with temperature control range from 25 to 100 °C and resolution of 0.1 °C. Figure 4 shows that both the PCF interferometer and LPG resonance wavelengths moved toward longer wavelengths linearly as temperature increased, giving temperature sensitivity of 10.4 and 47.4 pm/°C, respectively. The sensor matrix resulting from the aforementioned separate measurements with external RI and temperature can be obtained. By measuring the change in the resonance wavelengths of PCF and LPG, change in external RI and temperature can be measured simultaneously if the sensor works within a linear range as shown below:
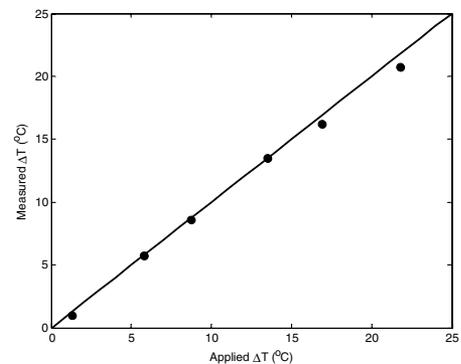

Fig. 3.   Spectral response of the sensor with external RI.

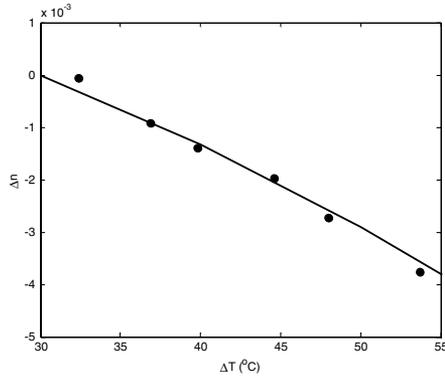Fig. 5.   Measured versus actual temperature shift ΔT.

Fig. 6.   Measured versus calibrated RI change Δn in [20].

$$\begin{bmatrix} \Delta n \\ \Delta T \end{bmatrix} = \begin{bmatrix} 171.96(\text{nm/RIU}) & 10.4 \times 10^{-3}(\text{nm/°C}) \\ -30.82(\text{nm/RIU}) & 47.4 \times 10^{-3}(\text{nm/°C}) \end{bmatrix}^{-1}$$
$$\times \begin{bmatrix} \Delta\lambda_{\text{PCF}} \\ \Delta\lambda_{\text{LPG}} \end{bmatrix}.$$

Next, the capability of the device for dual-parameter measurement was experimentally demonstrated and evaluated. The device was immersed in DI water which was heated in the oven from room temperature. A thermometer was used to monitor the temperature of the DI water continuously. Readings were taken at 31.2, 32.4, 36.9, 39.8, 44.6, 48.0, and 53.7 °C. The spectrum at 31.2 °C was used as the reference for comparison. The temperature shift and RI shift were determined from the sensor matrix and compared with the actual shifts as shown in Figs. 5 and 6. In Fig. 5, the solid line represents the perfect case when the measured temperature shift ΔT is the same as the applied temperature change ΔT. The solid circles represent the measured ΔT which agreed well with the actual ΔT. In Fig. 6, the solid line was obtained from the tabulated RI of water as a function of temperature (Table 7 in [20], measured at 0.1 MPa for wavelength 0.6382 μm). The RI at 30 °C was used as the reference value for comparison. The measured Δn showed acceptable agreement with [20], with less than 3×10^{-4} deviation.

In conclusion, a novel fiber sensor device based on LPG cascaded to PCF modal interferometer for simultaneous measurement of RI and temperature was developed and investigated. The cross-sensitivity was addressed effectively by producing a sensor matrix which was obtained by carrying out separate measurements with temperature and external RI. The implemented sensor demonstrated its capability in dual-parameter measurement. The simultaneous measurement of the temperature and external RI was experimentally demonstrated by the sensor and showed good agreement with actual values.

References

1. Y. Zhao, Y. Liao, B. Zhang, and S. Lai, J. Lightwave Technol. **21**, 1334 (2003).
2. L. Men, P. Lu, and Q. Chen, J. Appl. Phys. **103**, 053107 (2008).
3. K. Zhou, L. Zhang, X. Chen, and I. Bennion, Opt. Lett. **31**, 1193 (2006).
4. L. Rindorf and O. Bang, Opt. Lett. **33**, 563 (2008).
5. J. R. Ott, M. Heuck, C. Agger, P. D. Rasmussen, and O. Bang, Opt. Express **16**, 20834 (2008).
6. D. J. J. Hu, J. L. Lim, M. K. Park, L. T.-H. Kao, Y. Wang, H. Wei, and W. Tong, IEEE J. Sel. Top. Quantum Electron., "Photonic crystal fiber based interferometric biosensor for streptavidin and biotin detection" (to be published).
7. S. Y. Wu, H. P. Ho, W. C. Law, C. Lin, and S. K. Kong, Opt. Lett. **29**, 2378 (2004).
8. W. Yuan, H. P. Ho, C. L. Wong, S. K. Kong, and C. Lin, IEEE Sens. J. **7**, 70 (2007).
9. K. S. Park, H. Y. Choi, S. J. Park, U.-C. Paek, and B. H. Lee, IEEE Sens. J. **10**, 1147 (2010).
10. D. J. J. Hu, Y. Wang, J. L. Lim, T. Zhang, K. Mileńko, Z. Chen, M. Jiang, G. Wang, F. Luan, P. P. Shum, Q. Sun, H. Wei, W. Tong, and T. R. Woliński, IEEE Sens. J. **12**, 1239 (2012).
11. X. Shu, B. A. L. Gwandu, Y. Liu, L. Zhang, and I. Bennion, Opt. Lett. **26**, 774 (2001).
12. S.-M. Lee, S. S. Saini, and M.-Y. Jeong, IEEE Photon. Technol. Lett. **22**, 1431 (2010).
13. C. R. Liao, Y. Wang, D. N. Wang, and M. W. Yang, IEEE Photon. Technol. Lett. **22**, 1686 (2010).
14. P. Lu, L. Men, K. Sooley, and Q. Chen, Appl. Phys. Lett. **94**, 131110 (2009).
15. L. V. Nguyen, M. Vasiliev, and K. Alameh, IEEE Photon. Technol. Lett. **23**, 450 (2011).
16. D. W. Kim, F. Shen, X. Chen, and A. Wang, Opt. Lett. **30**, 3000 (2005).
17. A. P. Zhang, L.-Y. Shao, J.-F. Ding, and S. He, IEEE Photon. Technol. Lett. **17**, 2397 (2005).
18. Z. Zang and W. Yang, J. Appl. Phys. **109**, 103106 (2011).
19. H.-J. Kim, O.-J. Kown, S. B. Lee, and Y.-G. Han, Appl. Phys. B **102**, 81 (2011).
20. P. Schiebener, J. Straub, J. M. H. L. Sengers, and J. S. Gallagher, J. Phys. Chem. Ref. Data **19**, 677 (1990).